

Deformation-Induced Size Effects on the Structure and Mechanical Properties of Heterogenous PBF-LB/M AlSi10Mg Alloys

Extended Abstract

Introduction

The persistent demand for lightweight, high-performance materials in the aerospace and automotive industries has propelled the development and adoption of advanced manufacturing techniques. Laser-Based Powder Bed Fusion of Metals (PBF-LB/M), a prominent additive manufacturing (AM) process, offers the ability to fabricate geometrically complex components from high-strength aluminum alloys like AlSi10Mg. The PBF-LB/M process imparts a unique hierarchical microstructure to AlSi10Mg, characterized by a fine, interconnected network of eutectic Si within a ductile α -Al matrix. While this cellular architecture provides high strength, its inherent brittleness creates a fundamental strength-ductility trade-off, limiting its use in damage-tolerant structural applications. This research confronts this challenge by systematically investigating a multi-stage thermomechanical processing strategy designed to strategically tailor microstructural heterogeneity, control dislocation dynamics, and ultimately engineer an alloy with a superior combination of strength and ductility.

Methodology

This study integrates advanced manufacturing with targeted post-processing to control the alloy's microstructure across multiple length scales. AlSi10Mg samples were fabricated using PBF-LB/M. To create distinct initial microstructural states, the as-built samples were subjected to two low-temperature annealing (LTA) protocols: a short anneal at 280 °C for 9 minutes (LTA_280) and a longer anneal at 300 °C for 30 minutes (LTA_300). This created three starting conditions:

- As-built: Featuring a continuous, fine eutectic Si cellular network.
- LTA_280: Characterized by a partially ruptured Si network.
- LTA_300: Possessing a fragmented and spheroidized Si particulate structure.

The distinct difference between the as-built and the fully fragmented LTA_300 microstructures is visualized in the TEM results in Figures 1 and 2 respectively.

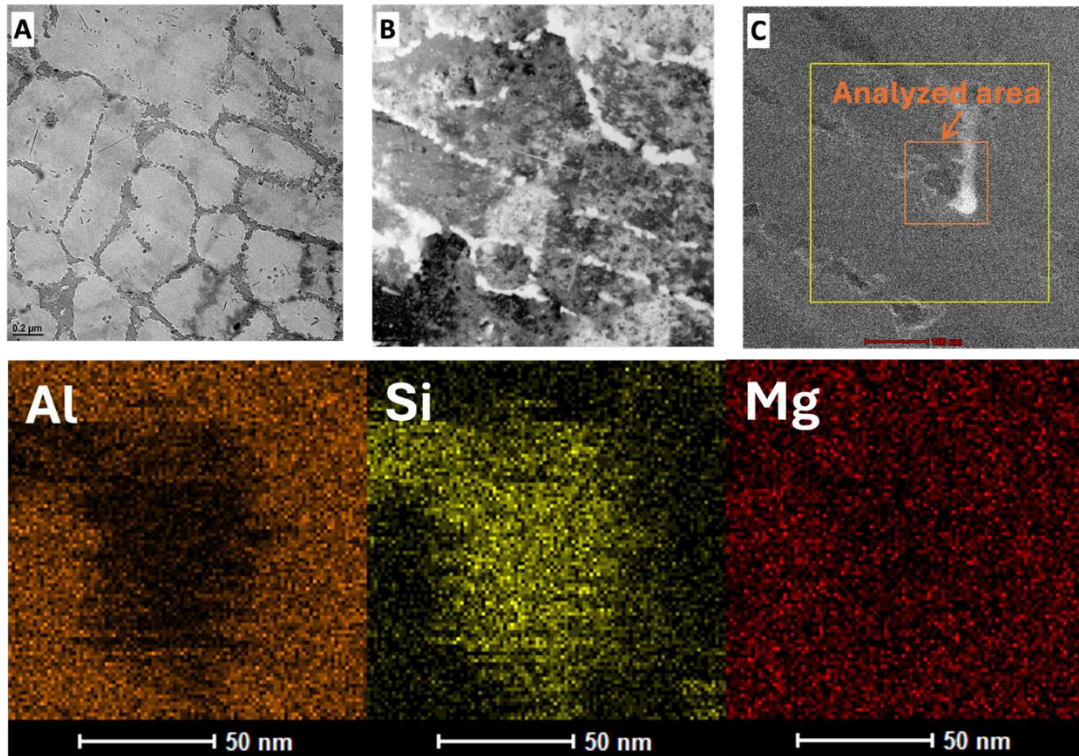


Figure 1. Cellular structure of As-built PBF-LB/M AlSi10Mg obtained from transmission electron microscopy (TEM) A. TEM image showing a magnified view of the full cellular structure, B. Higher magnification TEM image showing dislocation entanglements in the cell structure interiors, and C. STEM image and accompanying EDS mapping depicting Si segregation at the cell boundary.

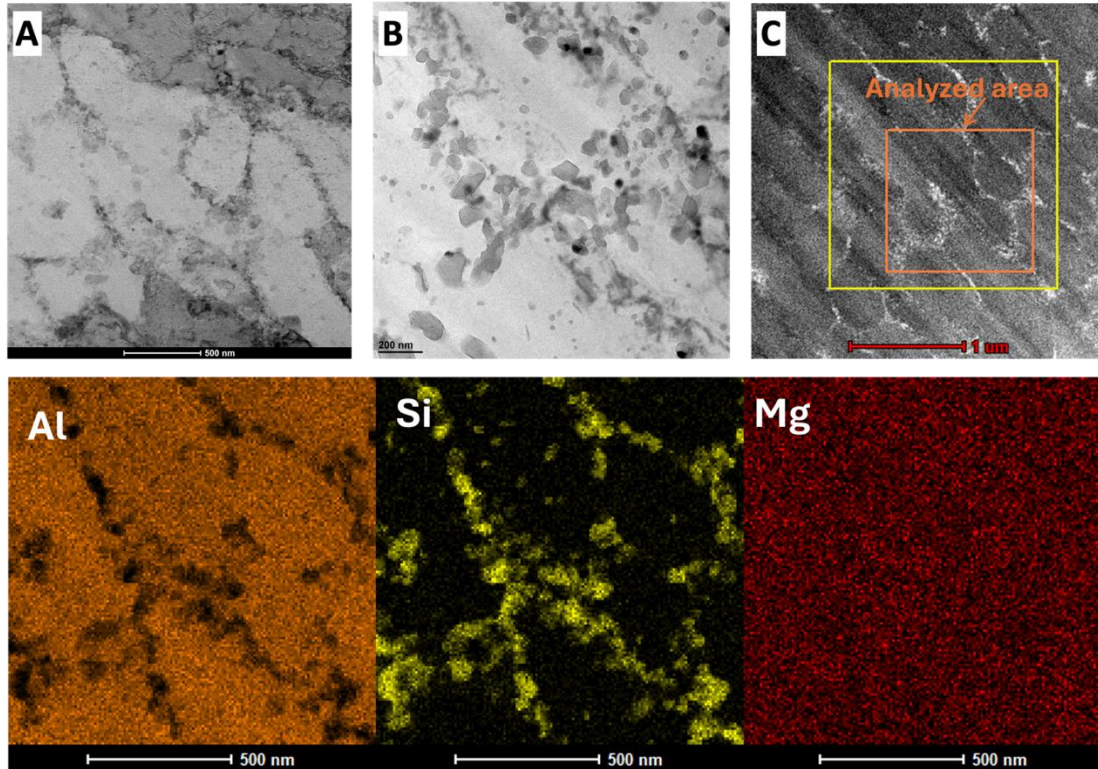


Figure 2. Cellular structure of LTA_300 obtained from transmission electron microscopy (TEM) A. TEM image showing the fragmented cellular structure, B. Higher magnification TEM image showing coarsened Si particles at the cell boundaries C. STEM image and accompanying EDS mapping of the fragmented cell boundaries.

Deformation Processing

These three conditioned sample sets were subjected to two modes of deformation:

- Gradual uniaxial compression: Samples were compressed to progressive strain levels (5%, 20%, and fracture) to study the fundamental evolution of the dislocation substructure.
- Severe plastic deformation (SPD): Samples were processed via equal channel angular pressing (ECAP) and twist channel angular pressing (TCAP) at various temperatures and passes to induce grain refinement and work hardening.

Multi-Scale Characterization

A comprehensive characterization suite – Including LOM, SEM, EDS, EBSD, TEM, XRD, and mechanical tests – was employed to establish a rigorous link between processing, microstructure,

and mechanical properties. Crucially, cyclic loading-unloading-reloading (LUR) tests were conducted to quantify kinematic hardening and the evolution of internal back stress.

Results and Discussion

The study revealed that the continuity of the eutectic Si network is the most dominant factor governing the alloy's mechanical response and its potential for optimization. The initial microstructural state dictates the primary strain hardening mechanism. The continuous Si network in the As-built sample creates significant plastic strain incompatibility between the hard Si and soft Al phases. This necessitates the generation of a high density of geometrically necessary dislocations (GNDs) to maintain lattice continuity at the Al/Si interface. This is confirmed by kernel average misorientation (KAM) analysis (Figure 3), which shows the highest GND accumulation in the As-built state after 5% strain.

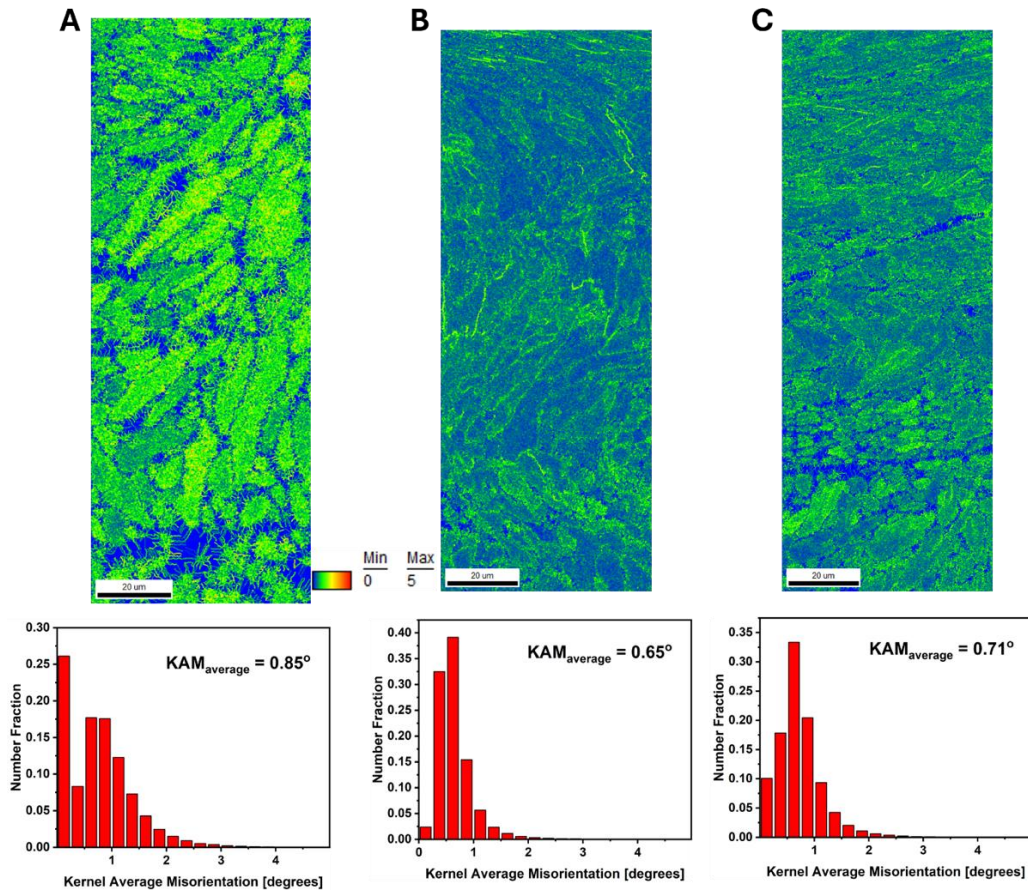


Figure 3. Kernel average misorientation (KAM) analysis of the samples after 5% strain compression A. As-built, B. LTA_280, and C. LTA_300

These GNDs generate powerful long-range internal back stresses, leading to significant kinematic hardening, which was measured to be as high as ~351 MPa post-ECAP (Figure 4). This GND-driven hardening provides high initial strength but also leads to intense stress concentrations at the network, causing premature fracture.

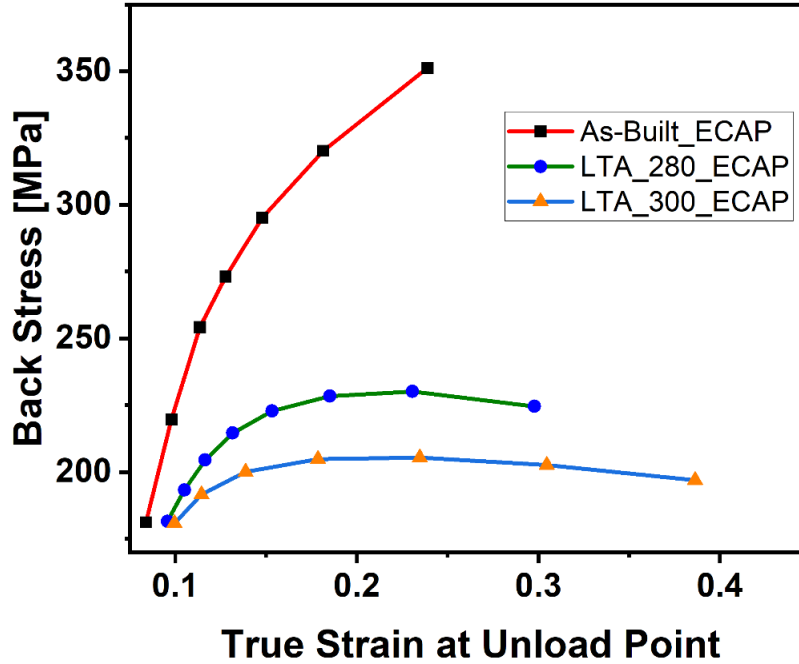


Figure 4. Back stress estimated from each LUR cycle for the ECAP-processed samples

In contrast, the LTA_300 treatment, by fragmenting the brittle network, fundamentally changes the deformation behavior. It enables more homogeneous deformation, which minimizes GND generation but unlocks high ductility in the α -Al matrix (failure strain increased from 35.1% to 47.2%). This allows for the extensive storage of statistically stored dislocations (SSDs) throughout the material, with densities reaching $1.48 \times 10^{14} \text{ m}^{-2}$ at fracture.

The study demonstrates that the success of SPD is critically dependent on this initial microstructural conditioning. Applying SPD to the brittle As-built material led to further embrittlement as the intense strain forcibly fractured the remaining network. Nonetheless, the key to achieving a superior property combination was applying SPD to the ductile, pre-conditioned LTA_300 material. This strategy leverages the pre-fragmented Si particles as stable sites for grain nucleation while the ductile matrix undergoes refinement and dislocation strengthening. The result is a material that has an appreciable combination of strength and ductility (Figure 5).

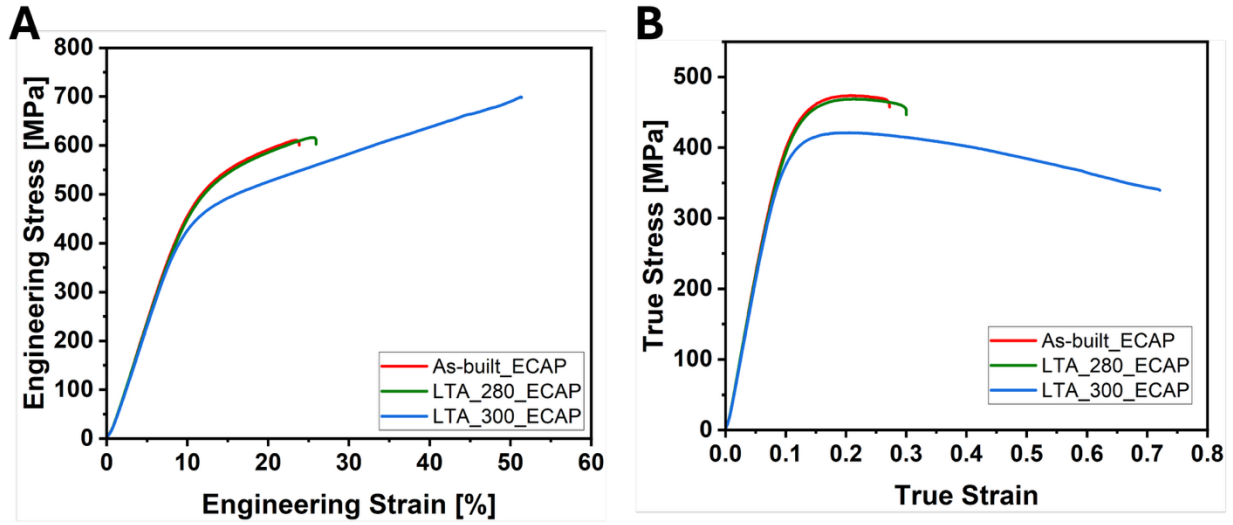


Figure 5. Engineering (A) and True (B) stress-strain plots of compressed ECAP-processed samples

Furthermore, a clear processing boundary was established: high-temperature ECAP (e.g. 350 °C) was found to be detrimental, causing catastrophic softening due to Si particle coarsening and dynamic recovery, erasing the unique benefits of the AM microstructure.

Conclusion and Significance

This thesis establishes a mechanism-based framework for designing high-performance, damage-tolerant AM alloys. The principal conclusion is that the paradoxical strength-ductility trade-off in PBF-LB/M AlSi10Mg can be overcome through a synergistic thermomechanical pathway:

- **Pre-conditioning:** An LTA treatment (300 °C for 30 minutes) is used to strategically fragment the brittle Si network, sacrificing some initial strength to unlock exceptional ductility.
- **Deformation:** Cold or warm SPD (e.g., TCAP) is then applied to the ductile material to induce massive grain refinement and dislocation strengthening.

This validated strategy produces a lightweight aluminum alloy with an excellent combination of yield strength and ductility, placing it in a competitive position for demanding aerospace and automotive applications.